Critical Residues Influence the Affinity and Selectivity of α-Conotoxin MI for Nicotinic Acetylcholine Receptors†

Richard B. Jacobsen, Richard G. DelaCruz, Julianne H. Grose, J. Michael McIntosh, Doju Yoshikami, and Baldomero M. Olivera*

Department of Biology, University of Utah, 257 South 1400 East, Salt Lake City, Utah 84112-0840

Received March 31, 1999; Revised Manuscript Received July 16, 1999

ABSTRACT: The mammalian skeletal muscle acetylcholine receptor contains two nonequivalent acetylcholine binding sites, one each at the α/δ and α/γ subunit interfaces. α-Conotoxin MI, a 14-amino acid competitive antagonist, binds at both interfaces but has ∼10^4 higher affinity for the α/δ site. We performed an "alanine walk" to identify the residues in α-MI that contribute to this selective interaction with the α/δ site. Electrophysiological measurements with *Xenopus* oocytes expressing normal receptors or receptors lacking either the γ or δ subunit were made to assay toxin−receptor interaction. Alanine substitutions in most amino acid positions had only modest effects on toxin potency at either binding site. However, substitutions in two positions, proline-6 and tyrosine-12, dramatically reduced toxin potency at the high-affinity α/δ site while having comparatively little effect on low-affinity α/γ binding. When tyrosine-12 was replaced by alanine, the toxin's selectivity for the high-affinity site (relative to that for the low-affinity site) was reduced from 45 000- to 30-fold. A series of additional amino acid substitutions in this position showed that increasing side chain size/hydrophobicity increases toxin potency at the α/δ site without affecting α/γ binding. In contrast, when tyrosine-12 is diiodinated, toxin binding is nearly irreversible at the α/δ site but also increases by ∼500-fold at the α/γ site. The effects of position 12 substitutions are accounted for almost entirely by changes in the rate of toxin dissociation from the high-affinity α/δ binding site.

The nicotinic acetylcholine receptor (nAChR)[1] is a key component of neuromuscular transmission. Not surprisingly, many animals that use venom to capture prey have evolved toxins to inhibit this critical locus. Among the most well-known of these venomous predators are the elapid snakes, including kraits, cobras, and sea snakes, which produce well-characterized toxins such as α-bungarotoxin, cobratoxin, and erabutoxin, respectively, all of which are potent competitive antagonists of muscle nAChRs (for an overview, see ref *1*). Another large group of animals that produce nicotinic antagonists is the venomous cone snails (*Conus* sp.) (*2*, *3*). These predatory marine mollusks have evolved very complex venoms, and every species of *Conus* examined so far produces an array of nAChR antagonists.

In the venoms of fish-hunting cone snails, which comprise about 70 of the 500 species of *Conus*, there appear to be two predominant groups of specialized nAChR antagonists that serve as primary paralytic toxins to immobilize prey. In fish-hunting species from the Eastern Pacific and Atlantic marine provinces, the αA-conotoxins, which have three disulfide linkages, are the primary venom components targeted to skeletal muscle nAChRs (*4*, *5*). On the other hand, most of the fish-hunting cone snails from the Indo-Pacific marine province have small peptide antagonists with a characteristic spacing between disulfide bonds—these are the α-conotoxins belonging to the "α3/5" subfamily, named for possessing intercysteine loop sizes of 3 and 5 amino acids (*2*); examples are shown in Table 1.

Table 1: Naturally Occurring α3/5-Conotoxins

toxin	sequence	ref
MI	GRCCHPACGKNYSC*	*26*
GI	ECCNPACGRHYSC*	*27*
SI	ICCNPACGPKYSC*	*28*
SIA	YCCHPACGKNFDC*	*29*
GIA	ECCNPACGRHYSCGK*	*27*
GII	ECCHPACGKHFSC*	*27*

Compared to other multiply disulfide-bonded peptides found in *Conus* venoms, the α3/5-conotoxins have a relatively narrow sequence range. Most fit the consensus sequence shown below:

$$XCC\begin{matrix}N\\H\end{matrix}PACG\begin{matrix}KNY\\RHF\end{matrix}SC\text{-}NH_2$$

Despite this tight consensus sequence, individual α-conotoxins from different fish-hunting species diverge considerably from each other, a common observation in *Conus* venom peptides. Two specific examples are α-SIA from *Conus striatus* and α-GI from *Conus geographus* (see Table 1); despite similar potencies, only a third of the non-cysteine amino acids are conserved between the two peptides. So far, the subfamily of competitive nAChR antagonists that fit the consensus sequence has been found exclusively in fish-

† This work was supported by the National Institutes of Health Grant GM 48677.

* To whom correspondence should be addressed: phone, (801)581-8370; fax, (801)585-5010; e-mail, oliveralab@bioscience.utah.edu.

[1] Abbreviations: ACh, acetylcholine; acm, *S*-acetamidomethyl; ACN, acetonitrile; fmoc, *N*-(9-fluorenyl)methoxycarbonyl; HPLC, high-performance liquid chromatography; nAChR, nicotinic acetylcholine receptor; TFA, trifluoroacetic acid.

10.1021/bi9907476 CCC: $18.00
Published on Web 09/11/1999

hunting cone snail venoms. The predominant α-conotoxins found in the venoms of non-fish-hunting *Conus* species do not fit the consensus sequence and primarily target neuronal subtypes of nAChRs.

The α3/5 subfamily of *Conus* peptides has among the most highly selective ligands known to target the mammalian skeletal muscle nAChR. α-Bungarotoxin from snake antagonizes both ACh binding sites of the mammalian nicotinic receptor (i.e., at both the α/δ and α/γ interfaces), as well as the homomeric α7 nAChRs (*6*, *7*). In contrast, the α3/5 subfamily of conotoxins is highly specific for the α/δ interface of the mammalian muscle nAChR; these peptides have affinities $>10^4$ lower for the α/γ interface (*8*−*10*) and $>10^5$ lower for the α7 neuronal nAChR (*11*), and they do not block any other known neuronal nAChR subtype when tested at concentrations up to 10 μM (*7*). The determinants on the α and δ subunits of the mammalian muscle nAChR that contribute to the binding of one member of the α3/5-conotoxin subfamily, α-MI, have been identified (*10*, *12*).

For *Torpedo* electric organ nAChRs, α-conotoxin selectivity is reversed, favoring the α/γ site (*13*, *14*). Recent studies have identified a basic amino acid in the second disulfide loop of α-GI, a highly conserved position in the α3/5 subfamily, as the selectivity determinant for *Torpedo* receptors (*15*, *16*). In the mouse muscle nAChR, however, this basic residue contributes similarly to binding at both interfaces (*15*), suggesting that a selectivity determinant is located elsewhere in the toxin sequence.

To address this unexplained selectivity and to gain a more complete picture of α-conotoxin interactions with the nAChR, we have investigated the functional consequences of amino acid substitutions in synthetic analogues of α-MI. The peptides were assessed by measuring their ability to block ACh-gated currents in *Xenopus* oocytes injected with cRNA encoding mouse muscle nAChR subunits.

MATERIALS AND METHODS

High-Performance Liquid Chromatography. All synthetic peptides were purified by preparative HPLC using Vydac C_{18} columns (22 mm × 25 cm, 15 μm particle size, 300 Å pore size, 20 mL/min flow rate). Analytical HPLC (Vydac C_{18} #218TP54; 4.6 mm × 25 cm, 5 μm particle size, 300 Å pore size, 1 mL/min flow rate) was used to monitor cleavage, iodination, and oxidation reactions (see below) as well as to assess the purity of fully oxidized peptides. Buffers consisted of 0.1% trifluoroacetic acid (TFA) in H_2O (buffer A) and 0.092% TFA and 60% acetonitrile (ACN) in H_2O (buffer B). Peptides were eluted using 10−40% linear gradients of B buffer over 30 min.

Peptide Synthesis. All peptides were built on Rink amide resin using standard fmoc (*N*-(9-fluorenyl)methoxycarbonyl) chemistry as previously described (*17*). The first and third cysteine residues in each peptide were *S*-trityl-protected; the second and fourth cysteines were protected with non-acid-labile *S*-acetamidomethyl (acm) groups. The remaining amino acids were protected as follows: pentamethylchromasulfonyl (Arg), *tert*-butyl (Asp, Ser, Tyr), *S*-trityl (Asn, His), *tert*-butoxycarbonyl (Lys, Trp).

The procedures for removing linear peptides from resin have been described previously (*5*, *17*, *18*). Peptides were oxidized using a two-step oxidation protocol similar to those detailed elsewhere (*17*, *19*). Initially, the first disulfide bridge of each peptide was closed by air oxidation. This protocol often involved incubation times of many days, and consequently an alternative strategy was adopted for oxidizing the first pair of cysteines.

Following preparative purification of the linear peptide, the HPLC eluant was added dropwise over several minutes to an equal volume of 20 mM $K_3Fe(CN)_6$ solution in 0.1 M Tris-base, pH 7.7, and stirred for 1 h. An Alltech extract-clean syringe containing C_{18} silica (1 g silica, 100 μm particle size, 60 Å pore size; catalog #215430) was wetted by gravity perfusion with buffer B (see HPLC methods for description of buffers) for ∼30 min followed by brief perfusion (1−2 min) with buffer A. The peptide oxidation mixture was diluted at least 2-fold with buffer A and passed through the silica under vacuum (flow rate ∼50 mL/min). The silica was then washed with ∼1 L of buffer A under vacuum until the yellow coloration caused by the $K_3Fe(CN)_6$ solution had cleared, and peptide was then eluted by gravity perfusion with 20 mL of buffer B. The removal of acm protection and the closure of the final disulfide were accomplished by oxidation with iodine (*17*). The tryptophan-containing α-MI analogue was oxidized with 2 mM iodine in 5% TFA for 5 min to minimize side reactions between tryptophan and iodine. Fully oxidized peptide was purified by preparative HPLC. Each synthesis was confirmed with liquid secondary ionization mass spectroscopy by Dr. Anthony Craig at the Salk Institute facility, La Jolla, CA.

Iodination of α-MI at Tyrosine-12. The tyrosine in position 12 of α-MI was selectively mono- and diiodinated by reaction with Iodogen (Pierce, catalog #28600). Tubes (15 mL, Sarstedt) were coated with Iodogen by gently vortexing 2 mL of 2 mg/mL Iodogen in chloroform until dry. Equimolar amounts (typically 200 nmol) of MI and NaI were combined (0.6 mL combined volume) in 2.7 mL of 0.3 M NH_4OAc (pH 5), vortexed for 5 min in the tube, extracted twice with 10 mL of ethyl acetate, and diluted 10-fold with HPLC buffer A before loading onto an HPLC column. The iodinated derivatives were separated by preparative HPLC using 10−50% gradient of buffer B over 40 min and confirmed by electrospray mass spectrometry at the University of Utah core facility.

Recordings from Acetylcholine Receptors Expressed in Oocytes. Oocyte harvesting from *Xenopus* frogs, preparation, and injection were performed as previously described (*17*). Equal quantities of cRNA encoding the embryonic mouse muscle α1, β1, γ, and δ subunits as derived from BC_3H-1 cells were co-injected to provide receptors with $(\alpha1)_2\beta1\gamma\delta$ stoichiometry ("wild-type" receptors); co-injection of α1, β1, and γ cRNA provided receptors with $(\alpha1)_2\beta1\gamma_2$ ("αβγ" receptors) stoichiometry; and α1, β1 and γ cRNA were co-injected to produce receptors with $(\alpha1)_2\beta1\delta_2$ ("αβδ" receptors) stoichiometry (*20*; also see ref *5*). Voltage-clamp assays of oocytes were performed 1−3 days following injection for wild-type receptor and after 3−7 days for αβγ and αβδ receptors. Voltage-clamping, toxin and ACh perfusion, and buffers were as described previously (*5*, *21*) except for the modifications below.

An injected oocyte was placed in a rectangular recording chamber (∼1 mL volume) fabricated from Sylgard and gravity-perfused with buffer at a rate of ∼3 mL/min. Pulses of ACh (typically 1 or 10 μM and 0.5−1 s in duration) were

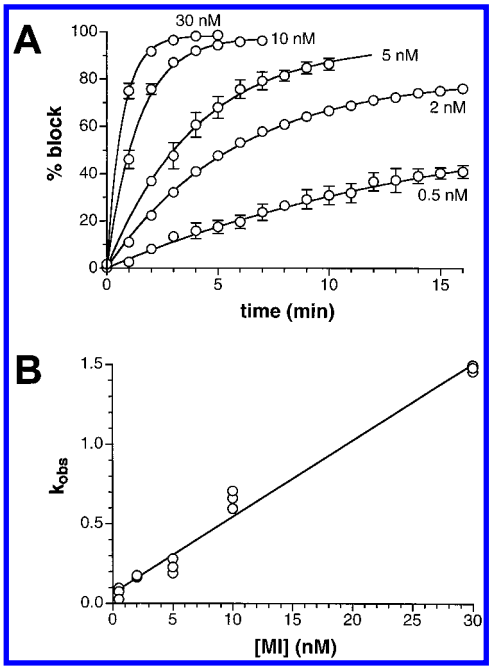

FIGURE 1: Kinetics of α-conotoxin MI block of mouse muscle nAChRs expressed in *Xenopus* oocytes. Responses to 1 s pulses of ACh applied at 1 min intervals were measured by voltage clamping. A. The time course of blockade was measured for five toxin concentrations. The ratio of control ACh-gated currents to those during toxin application, I/I_o, was used to calculate the percent block as follows: % block = $(1 - I/I_o) \times 100$. Solid lines are best-fit curves for averaged data using the equation: % block = $100 \times (1 - e^{-k_{obs}t})$ ($n = 3-4$, error bars represent SEM). B. Plot of k_{obs} vs MI concentration. Each point represents the k_{obs} for an individual wash-in experiment. The solid line represents that best fit to the equation: $k_{obs} = k_{on}[\text{toxin}] + k_{off}$. The rate constants k_{on} and k_{off} were calculated from the slope and intercept of the line, respectively.

applied at 1 min intervals. In most cases, each ACh pulse was followed by a 1−3 s "chase" pulse of ACh-free buffer from an additional reservoir to minimize the discrepancies caused by flow rate variations between toxin-containing reservoirs. Due to the slow off-rates of α-conotoxins, unbinding of toxin during the relatively brief ACh and chase pulses did not alter the apparent affinity or kinetics of the toxins (data not shown).

RESULTS

Electrophysiological Characterization of α*-Conotoxin MI.* The functional activity of α-MI was assessed by measuring its ability to block ACh-gated currents in oocytes expressing mouse wild-type nAChRs. The dissociation of α-MI was extremely slow; complete recovery of receptor function following equilibrium blockade required over 70 min of wash. As an alternative to directly measuring wash-out kinetics, we measured the rate of toxin wash-in (k_{obs}) at several concentrations, as shown in Figure 1A. For the lower concentrations, where equilibrium blockade could not be reached within the time frame of a typical experiment, the k_{obs} was estimated from the initial rate of receptor blockade. The k_{obs} was plotted against toxin concentration to obtain both association and dissociation constants as shown in Figure 1B (*22*). The apparent K_d of α-MI calculated from these kinetic parameters was in reasonable agreement with the IC_{50} determined from the fraction of receptors remaining active at equilibrium (see Table 2).

Table 2: IC_{50} Values and Kinetic Parameters for α-Conotoxin MI and Analogues on Wild-Type Receptors

toxin[a]	IC_{50}[b] (nM)	apparent K_d[c] (nM)	$k_{on} \times 10^7$ (M^{-1} min^{-1})	k_{off} (min^{-1})
α-MI	0.4 ± 0.01	1.4 ± 0.1	4.79 ± 0.18	0.066 ± 0.025
R2A	1.4 ± 0.2			
H5A	1.2 ± 0.1			
P6A	29 ± 2	69 ± 13	0.91 ± 0.15	0.52 ± 0.07
K10A	3.7 ± 0.3			
N11A	1.3 ± 0.1			
Y12A	3400 ± 410			
Y12M	19 ± 3	32 ± 12	5.01 ± 2.66	1.62 ± 0.32
Y12H	13 ± 1	11 ±. 0.5	5.61 ± 1.41	0.64 ± 0.03
Y12W	1.8 ± 0.2			
Y12Y−I_2	<0.4			
S13A	0.4 ± 0.1			
C*14C^	2.4 ± .0.4			

[a] Y12Y−I_2, diiodotyrosine-12 substitution; C*14C^, amide to free carboxy C-terminus. [b] IC_{50} is a measure of the functional block of receptor by toxin and was estimated from the fraction of active receptors at equilibrium (fraction active = 1/1 + ([toxin]/IC_{50}). The IC_{50}'s were calculated for individual experiments, typically using several toxin concentrations, and averaged. Errors are the SEM, $n = 3-7$. [c] K_d estimated from k_{off}/k_{on} obtained as described in Figure 1 for α-MI. Errors are the SEM, $n = 3-5$.

At the concentrations of α-MI used above, only the high-affinity binding site at the α/δ interface would be significantly blocked. To address the selectivity of α-MI in our oocyte expression system, we expressed nAChRs lacking either the γ or δ subunit. These functional receptors contain a single type of interface binding site and $(\alpha1)_2\beta1\delta_2$ or $(\alpha1)_2\beta1\gamma_2$ stoichiometry, respectively (*20*). As shown in Figure 2, α-MI distinguishes markedly between these receptors. The αβγ receptor was inhibited 25% by 10 μM α-MI (Figure 2B), while the αβδ receptor was inhibited more than 75% by 1 nM α-MI (Figure 2A). The IC_{50}'s for α-MI at the two binding sites (0.4 nM at the α/δ site, based on blockade of wild-type and αβδ receptors, and 18 μM at the α/γ site, based on blockade of αβγ receptors) differ by 45 000-fold (see Table 3).

Alanine Walk" of α*-MI.* We chemically synthesized analogues of α-MI with alanine substitutions in each non-cysteine amino acid position and examined their ability to block the function of the wild-type receptor. These results are summarized in Table 2. The effects of alanine substitution at most loci were relatively modest, ranging from no change (S13A) to a 9-fold loss of activity (K10A). As with the native toxin, the off-rates of these analogues were too slow to measure accurately; thus, for most analogues only an IC_{50}, based on the fraction of active receptors at equilibrium blockade, is reported. When equilibrium was not reached during an experiment, the level of equilibrium blockade was estimated from the rate of approach to equilibrium fit with a single exponential. The approach to, or achievement of, equilibrium blockade during wash-in of α-MI and several analogues that exhibited only slight changes in potency are shown for representative experiments in Figure 3A. An example of the extremely slow wash-out kinetics of α-MI and the N11A analogue are shown in Figure 4A.

Two Ala-substituted analogues, P6A and Y12A, exhibited dramatic reductions in IC_{50} (73- and 8 500-fold, respectively). The large effect of Y12A substitution led us to focus on the interactions of position 12 with the receptor through a series of additional substitutions. We synthesized analogues with

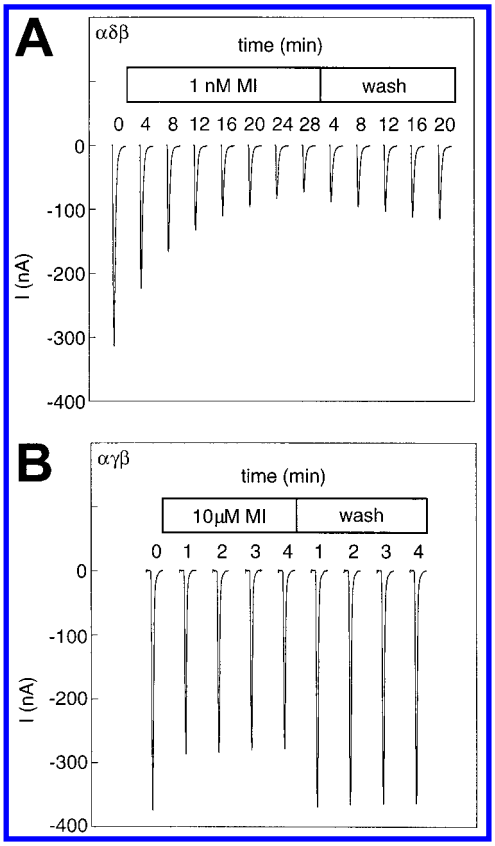

FIGURE 2: Comparison of α-MI's ability to block nAChRs lacking either the δ or γ subunit. α-MI blocked αβδ vs αβγ nAChRs with >20 000-fold higher potency. Each trace represents the response to a 1 s pulse of 10 μM ACh at the time (in min) indicated above the trace. Each trace is 15 s in duration. Toxin solution (at concentration indicated in box) was applied for the indicated duration starting at time = 0 and followed by perfusion with toxin-free buffer over the period indicated by the box labeled "wash". Panel A, αβδ receptors. Panel B, αβγ receptors.

Table 3: Approximate IC_{50} Values of α-MI and Analogues on αβγ and αβδ nAChRs

	αβγ		αβδ	
toxin	IC_{50}[a,b] (μM)	αβγ/wt[c]	IC_{50}[a,b] (nM)	αβδ/wt[d]
α-MI	18 ± 5	45 000	0.40 ± 0.17	1.0
R2A	103 ± 36	74 000	1.8 ± 0.3	1.3
H5A	36 ± 9	30 000	0.97 ± 0.44	0.8
P6A	129 ± 32	4 000	19 ± 2	0.7
K10A	118 ± 12	32 000	3.5 ± 1.5	0.9
N11A	21 ± 1	16 000	1.3 ± 0.1	1.0
Y12A	109 ± 15	30	3300 ± 400	1.0
Y12W	58 ± 12	32 000	1.5 ± 0.2	0.8
Y12M	10 ± 2	500	46 ± 7	2.4
Y12H	52 ± 13	4 000	35 ± 7	1.5
diiodoY12	0.04	na	na	na
S13A	10 ± 2	25 000	0.74 ± 0.09	1.9

[a] The IC_{50} was estimated from the fraction of active receptors as described in Table 2. [b] n = 3−6, except diiodoY12, which was estimated from a dose−response curve (not shown); errors are the SEM. [c] Calculated as IC_{50} αβγ/IC_{50} wild-type; see Table 2 for wild-type IC_{50}. [d] Calculated as IC_{50} αβδ/IC_{50} wild-type. na, could not be calculated due to apparently irreversible binding to αβδ and wild-type receptors.

Met, His, Trp, monoiodoTyr, and diiodoTyr in place of tyrosine-12. While the effects on IC_{50} and off-rate varied greatly among these analogues, all were more potent than the Y12A analogue, with the diiodinated derivative showing the highest affinity (see Table 2, Figures 3B and 4B). Due to an increase in off-rate, the Y12M and Y12H analogues

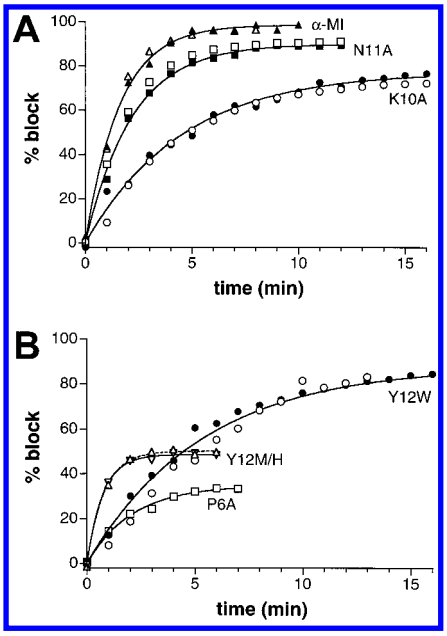

FIGURE 3: Wash-in of α-MI and analogues on wild-type (open symbols) and αβδ (closed symbols) nAChRs. A. Representative experiments showing the wash-in of 10 nM α-MI and analogues. The k_{obs} values (in min^{-1}) are as follows: α-MI (triangles, 0.62), N11A (circles, 0.46), K10A (squares, 0.23). B. Representative experiments showing the wash-in of Y12W for both wild-type and αβδ receptors and of the Y12M, Y12H, and P6A analogues on the wild-type receptor. The wash-in curves for Y12M/H at this concentration cannot be measured accurately due to rapid kinetics; estimated fits are shown for comparative purposes. Kinetics on the αβδ receptor are similarly fast and were omitted for figure clarity. The k_{obs} values (in min^{-1}) are as follows: Y12W (circles, 0.11), Y12H (triangles, broken line, 1.35), Y12M (inverted triangles, solid line, 1.35), and P6A (squares, 0.48). All curves were generated using a single-exponential function, and k_{obs} and % block were calculated as in Figure 1.

were the least potent (IC_{50} increased by about 50- and 30-fold, respectively) after Y12A, which exhibited dissociation kinetics too fast to measure in our system. The larger substitutions caused either no change (Y12W) or an increase in potency (the iodinated derivatives). The iodinated analogues take longer than the wild-type toxin to dissociate, with the diiodotyrosine causing block that showed no recovery following 30 min of wash (in two experiments, see Figure 4B). Thus, the more bulky the side chain in position 12 the more potent the toxin, with changes in apparent K_d manifested largely through changes in dissociation rate.

The only other alanine-substituted analogue with a dissociation rate that differed notably from that of the natural toxin is P6A, whose wash-in and wash-out are also shown in Figures 3B and 4B, respectively.

Selectivity: Activity of Analogues on αβγ and αβδ Receptors. We found that all analogues behaved similarly on αβδ and wild-type receptors; wash-in of the K10A and N11A analogues are compared for the two receptors in Figure 3A. The similarities between blockade of αβδ and wild-type receptors for most analogues are clear from the last column in Table 3; typically, the IC_{50} ratio for αβδ/wild-type was near 1. As shown in Table 3, the effects of alanine substitution in positions 6 and 12 were by far the most pronounced on both types of receptors.

In contrast, when α-MI analogues were tested on αβγ receptors, we found that nearly all substitutions had only

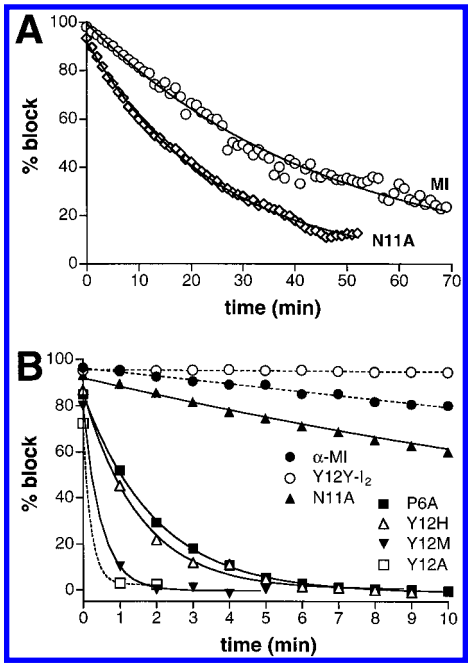

FIGURE 4: Dissociation rates of α-MI and analogues on wild-type nAChRs. A. Recovery from block following wash-out of MI (points are the average of four experiments) and N11A (single experiment). Curves were fit to a single exponential to determine k_{off}: 0.024 ± 0.004 min^{-1} for MI (average of individual k_{off} values for four experiments) and 0.040 min^{-1} in the single N11A experiment. B. Representative experiments in which the toxins indicated in the legend were applied until equilibrium blockade was achieved and then washed out beginning at time = 0. While an Ala substitution in position 12 (Y12A) accelerated the wash-out time to <1 min (squares connected by broken line), diiodination of Tyr-12 (Y12Y-I_2) produced nearly irreversible block. In general, increasing the size of the side chain of the residue in position 12 decreased the dissociation rate, as seen from Met and His substitutions. Proline-6 is also important for toxin binding; alanine substitution in this position increases the dissociation rate 10−20-fold. Data points were fit to a single exponential (lines) to determine k_{off} values (in min^{-1}) of N11A (0.04), P6A (0.54), Y12H (0.65), Y12M (2.03), and Y12A (>4.5). See Figure 1 for a description of % block.

minor effects on potency (reductions ranging from 0- to 6-fold, Table 3). These observations are interesting in that even alanine substitution for Y12, which caused a $>10^3$ reduction in potency for wild-type receptors, results in only a 5-fold decrease in potency for $\alpha\beta\gamma$ receptors. The iodotyrosine derivatives were an unexpected exception to this trend, showing striking increases in potency for $\alpha\beta\gamma$ receptors, by about 500-fold for the diiodotyrosine derivative. Figure 5 is a comparison of representative experiments showing effects of α-MI, Y12A, and Y12Y-I_2 application to these receptors. We note that for α-MI and all analogues except the iodinated derivatives, the wash-in and wash-out kinetics on $\alpha\beta\gamma$ receptors were too fast to measure in our system (i.e., equilibrium was reached in less than 1 min).

DISCUSSION

Structure−Activity of α*-MI.* Most of the α-conotoxins listed in Table 1 exhibit marked discrimination between the α/δ and α/γ subunit interfaces of mouse muscle (*8*, *9*) and *Torpedo* electric organ (*13*) nAChRs. Our results identify the conserved aromatic residue in the second loop, which is either tyrosine or phenylalanine in all naturally occurring α3/5 conotoxins, as the major determinant of selectivity for

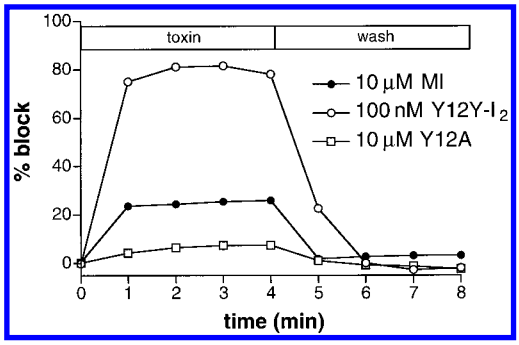

FIGURE 5: Potency of Y12-substituted peptides for $\alpha\beta\gamma$ nAChRs. Diiodination of tyrosine-12 increased the potency of MI for $\alpha\beta\gamma$ receptors. In contrast to results with the wild-type receptor, alanine substitution at this position produced only modest reduction in toxin potency on $\alpha\beta\gamma$ receptors. See Figure 1 for a description of % block.

the α/δ site on the mammalian receptor. Alanine substitution for tyrosine-12 (Y12) causes a slight (5-fold) loss of potency for the α/γ site but reduces potency for the preferred site by around 8500-fold.

We investigated the interaction of Y12 with the α/δ binding site through the use of a series of analogues with increasingly bulky side chains substituted for Y12. The hierarchy of affinities in this series of substitutions can be summarized as follows (see Table 2):

$$\text{Ala} << \text{Met} < \text{His} < \text{Trp} \approx \text{Tyr} < \text{diiodoTyr}$$

We should note that, with the exception of diiodotyrosine (discussed below), these substitutions had minimal effects on α/γ potency. Thus, any hydrophobic residue of sufficient size can restore some selectivity for the α/δ binding site. The surprising increase in potency following diiodination of tyrosine further suggests that a relatively nonspecific hydrophobic interaction can take place between toxins and the α/δ receptor interface. That iodination also increases activity at the α/γ binding site might indicate that the additional hydrophobicity and bulk of a diiodotyrosine allows better interaction with a hydrophobic binding pocket on the receptor, either directly or through a reorientation/shifting of the bound toxin.

Finally, we note that the 75-fold loss of potency for the α/δ site caused by an alanine substitution for proline-6 is different from the position 12 substitutions. Unlike the latter, which affected mainly the rate of toxin dissociation from the α/δ binding site, the P6A substitution altered both association and dissociation rates (see Table 2).

Implications for Toxin−Receptor Interaction. The tenable models for α-MI selectivity are narrowed by the discovery that peptides with a range of side chain size and aromatic character at position 12 still retain selectivity. Thus, specific hydrogen-bonding interactions or a tight lock-and-key model does not appear to fit the data; clearly, a variety of side chain residues confer selectivity for the α/δ vs α/γ interface, making highly specific interactions between Y12 and residues on the receptor less likely. Methionine or histidine substitutions at position 12 reduce potency primarily through changes in off-rates, with little change in on-rates, indicating that the initial contacts between peptide and receptor are not determined by the residues at this position. Rather, a highly aromatic residue at position 12 such as tyrosine or tryptophan anchors the peptide to the receptor, suggesting interaction

with a general hydrophobic pocket. This is consistent with a previous study by Hashimoto et al. in which a phenylalanine residue in this position was sufficient to maintain toxin potency (*23*). Loss of aromatic character or substitution of a smaller residue such as histidine at position 12 reduces this anchoring capacity. The ability of the diiodotyrosine derivative to slow the rate of peptide dissociation from the receptor further indicates that an interaction with a highly specific geometry, such as that required in a lock-and-key model, does not apply here.

However, this and previous results suggest that high affinity for the α/δ site requires the aromatic residue in position 12 to have the appropriate orientation. The only α-conotoxin in Table 1 that is not strongly selective for the α/δ site is α-SI; this peptide contains a proline in place of the conserved basic residue in the second disulfide loop (corresponding to lysine-10 in α-MI and arginine-9 in α-GI). It was suggested by Groebe et al. (*15*) that this peptide showed comparatively little selectivity due to a disruption of secondary structure in the second disulfide loop, rather than to any specific interactions. Replacing this proline with a lysine increased the selectivity of α-SI from 220- to 47 000-fold at the mouse receptor through enhancement in binding to the high-affinity site. However, our current findings agree with the suggestion by Groebe and co-workers that it is not the presence of a positively charged amino acid that accounts for the increased selectivity on the mouse receptor (since alanine at this position in MI has no effect on selectivity). We suggest, then, that the orientation of the tyrosine residue at position 12 is important in selectivity and that the proline residue in α-SI causes the tyrosine residue to be displaced from its optimal orientation. It is notable in this regard that in previous studies a D-tyrosine substitution at this position rendered both α-MI and α-GI inactive at all concentrations tested (*23*, *24*). A recently obtained ^{1}H NMR structure of α-MI has Y12 exposed to the solvent, well-positioned to anchor the toxin to the receptor (*25*).

REFERENCES

1. (1991) *Handbook of Natural Toxins. Reptile Venoms and Toxins*, Vol. 5, Marcel Dekker Inc., New York.
2. McIntosh, J. M., Santos, A. D., and Olivera, B. M. (1999) *Annu. Rev. Biochem.* (in press).
3. Olivera, B. M. (1997) *Mol. Biol. Cell 8*, 2101−2109.
4. Hopkins, C., Grilley, M., Miller, C., Shon, K., Cruz, L. J., Gray, W. R., Dykert, J., Rivier, J., Yoshikami, D., and Olivera, B. M. (1995) *J. Biol. Chem. 270*, 22361−22367.
5. Jacobsen, R., Yoshikami, D., Ellison, M., Martinez, J., Gray, W. R., Cartier, G. E., Shon, K., Groebe, D. R., Abramson, S. N., Olivera, B. M., and McIntosh, J. M. (1997) *J. Biol. Chem. 272*, 22531−22537.
6. Séguéla, P., Wadiche, J., Dineley-Miller, K., Dani, J. A., and Patrick, J. W. (1993) *J. Neurosci. 13*, 596−604.
7. Johnson, D. S., Martinez, J., Elgoyhen, A. B., Heinemann, S. S., and McIntosh, J. M. (1995) *Mol. Pharmacol. 48*, 194−199.
8. Kreienkamp, H.-J., Sine, S. M., Maeda, R. K., and Taylor, P. (1994) *J. Biol. Chem. 269*, 8108−8114.
9. Groebe, D. R., Dumm, J. M., Levitan, E. S., and Abramson, S. N. (1995) *Mol. Pharmacol. 48*, 105−111.
10. Sine, S. M., Kreienkamp, H.-J., Bren, N., Maeda, R., and Taylor, P. (1995) *Neuron 15*, 205−211.
11. Quiram, P. A., and Sine, S. M. (1998) *J. Biol. Chem. 273*, 11007−11011.
12. Sugiyama, N., Marchot, P., Kawanishi, C., Osaka, H., Molles, B., Sine, S. M., and Taylor, P. (1998) *Mol. Pharmacol. 53*, 787−794.
13. Hann, R. M., Pagán, O. R., and Eterovic, V. A. (1994) *Biochemistry 33*, 14058−14063.
14. Utkin, Y. N., Kobayashi, F. H., and Tsetlin, V. I. (1994) *Toxicon 32*, 1153−1157.
15. Groebe, D. R., Gray, W. R., and Abramson, S. N. (1997) *Biochemistry 36*, 6469−6474.
16. Hann, R. M., Pagán, O. R., Gregory, L. M., Jácome, T., and Eterovic, V. A. (1997) *Biochemistry 36*, 9051−9056.
17. Cartier, G. E., Yoshikami, D., Gray, W. R., Luo, S., Olivera, B. M., and McIntosh, J. M. (1996) *J. Biol. Chem. 271*, 7522−7528.
18. Shon, K., Grilley, M. M., Marsh, M., Yoshikami, D., Hall, A. R., Kurz, B., Gray, W. R., Imperial, J. S., Hillyard, D. R., and Olivera, B. M. (1995) *Biochemistry 34*, 4913−4918.
19. Monje, V. D., Haack, J., Naisbitt, S., Miljanich, G., Ramachandran, J., Nasdasdi, L., Olivera, B. M., Hillyard, D. R., and Gray, W. R. (1993) *Neuropharmacology 32*, 1141−1149.
20. Sine, S. M., and Claudio, T. (1991) *J. Biol. Chem. 266*, 19369−19377.
21. Cartier, G. E., Yoshikami, D., Luo, S., Jacobsen, R., Hunter, E. M., Shon, K., Olivera, B. M., and McIntosh, J. M. (1997) *J. Neurosci. Abstr. 23*, 384.
22. Taylor, P. (1990) in *Goodman and Gilman's The Pharmacological Basis of Therapeutics* (Gilman, A. G., Rall, T. W., Nies, A. S., and Taylor, P., Eds.) pp 166−186, Pergamon Press, New York.
23. Hashimoto, K., Uchida, S., Nishiuchi, Y., Sakaibara, S., and Yukari, K. (1985) *Eur. J. Pharmacol. 118*, 351−354.
24. Almquist, R. G., Kadambi, S. R., Yasuda, D. M., Weitl, F. L., Polgar, W. E., and Toll, L. R. (1989) *Int. J. Pept. Protein Res. 34*, 455−462.
25. Gouda, H., Yamazaki, K., Hasegawa, J., Kobayashi, Y., Nishiuchi, Y., Sakakibara, S., and Hirono, S. (1997) *Biochim. Biophys. Acta 1343*, 327−334.
26. McIntosh, J. M., Cruz, L. J., Hunkapiller, M. W., Gray, W. R., and Olivera, B. M. (1982) *Arch. Biochem. Biophys. 218*, 329−334.
27. Gray, W. R., Luque, A., Olivera, B. M., Barrett, J., and Cruz, L. J. (1981) *J. Biol. Chem. 256*, 4734−4740.
28. Zafaralla, G. C., Ramilo, C., Gray, W. R., Karlstrom, R., Olivera, B. M., and Cruz, L. J. (1988) *Biochemistry 27*, 7102−7105.
29. Myers, R. A., Zafaralla, G. C., Gray, W. R., Abbott, J., Cruz, L. J., and Olivera, B. M. (1991) *Biochemistry 30*, 9370−9377.

BI9907476